A coherent positron beam for reflection high-energy positron diffraction

A. Kawasuso,[a] T. Ishimoto, M. Maekawa, Y. Fukaya, K. Hayashi, and A. Ichimiya
Advanced Science Research Center, Japan Atomic Energy Research Institute, 1233, Watanuki, Takasaki, Gunma 370-1292, Japan

(Received 20 April 2004; accepted 15 August 2004; published 29 October 2004)

A 10 keV positron beam has been developed using coaxially symmetric electromagnetic lenses for reflection high-energy positron diffraction (RHEPD) experiments. The beam brightness is $\sim 10^7$ $e^+/s/cm^2/rad^2/V$ which is comparable to that obtained using brightness enhancement technique. The beam parallel and normal coherence lengths are over 100 and 40 Å, respectively, which are long enough to observe diffraction patterns associated with large surface super-structures. RHEPD patterns from a Si(111)-(7×7) reconstructed surface have been successfully observed with a much better quality than previously reported. © *2004 American Institute of Physics.*
[DOI: 10.1063/1.1806651]

I. INTRODUCTION

Reflection high-energy positron diffraction (RHEPD) has emerged as a powerful tool to investigate atomic structures and vibrational states associated with solid surfaces.[1,2] As compared to conventional electron diffraction, one major advantage of this method is the appearance of the total reflection of positrons.[3] Incident positrons are completely reflected at the first surface layer, with negligible penetration into the bulk, when the glancing angle is lower than the critical angle. This implies that the sensitivity of the diffraction intensity to the first surface layer is fairly enhanced.

To realize RHEPD observations, a small diameter and a highly parallel positron beam is required. This corresponds to the reduction of the phase space area occupied by positrons. According to Liouville's theorem, by increasing the beam energy, the phase space area can be sufficiently reduced. There are two ways to generate such a coherent positron beam. One way is to use electrostatic lenses and the other way is to use electromagnetic lenses. In our previous research, we developed an electrostatic beam apparatus by combining a modified Soa gun and Einzel lenses.[4–7] The modified Soa gun is well suited to transport the beam, which initially has a relatively large angular spread ($\Delta\theta\sim10°$). Since the tight beam focus causes an increase in the angular spread, only the paraxial beam was extracted using a pinhole collimator under a relatively weak focus condition. By doing so, the RHEPD observation was carried out successfully.

In recent times, it has been reported that even by the combination of an aperture electrode and a tube lens, a well-focused, high-energy positron beam can be formed with an ample angular acceptance.[8] This implies that the modified Soa gun may be replaced with such a method. Although a high-energy positron beam used in RHEPD experiments can, in principle, be generated using the above electrostatic apparatus, such a system has been originally used in low-energy region and is not necessarily suitable for high-energy beam optics. General disadvantages of the electrostatic lens, in comparison with the electromagnetic lens are (i) its relatively large aberrations, (ii) nonselectivity for positive particles with different masses, and (iii) strong dependence of the lens field on the beam energy. For generation of a high-energy positron beam, the electromagnetic lens is more convenient than the electrostatic lens. In this study, we developed a positron beam apparatus with a gun fabricated using multiple immersion lenses and with a transport system composed of coaxial electromagnetic lenses.

II. INSTRUMENT

A common theme of any beam development processes is to enhance the brightness. For this purpose, the so-called brightness enhancement technique was proposed.[9] The most primitive method of brightness enhancement is the moderation of fast positrons emitted from a radioactive source. In principle, the brightness can be further enhanced using the second or further remoderation stages. This may be indispensable while generating positron microbeams or highly monochromatic low-energy positron beams. However, our aim here is to create a high-energy positron beam which is suitable for diffraction experiments. Considering the advantage that the beam transport in high-energy region (>10 keV) is much more convenient than in low-energy regions, we may not employ the brightness enhancement technique with the exception of the primary moderation. It has been proven that a positron beam with adequate brightness could be obtained in the following manner. From Liouville's theorem, the normalized emittance of a beam ($\varepsilon_{\mathrm{norm}}$) is conserved.[10] That is, assuming uniform moderator with a radius of r_m:

$$\varepsilon_{\mathrm{norm}} = 4r_m\sqrt{\Phi_m}\tan\theta_m = 4r\sqrt{\Phi}\tan\theta, \tag{1}$$

where Φ_m is the effective acceleration voltage due to the negative work function of the moderator, and θ_m is the angular spread of positrons emitted from the moderator. Also, r and θ are the beam radius and angular spread due to the acceleration voltage of Φ. The emittance (i.e., the area on

[a]Author to whom correspondence should be addressed; electronic mail: ak@taka.jaeri.go.jp

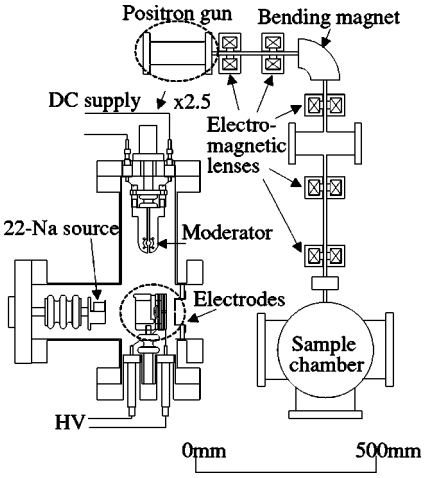

FIG. 1. Schematic diagram of the positron beam apparatus.

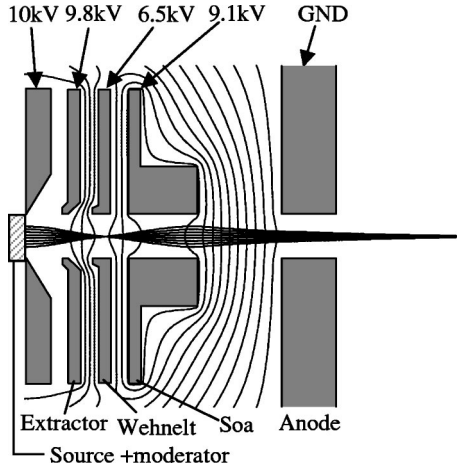

FIG. 2. Beam trajectories simulated by the SIMION program. The electrostatic potentials at the moderator and the other electrodes are also shown. The initial positron energy from the moderator is 3 eV. The contour spacing of the electrostatic potential is 1 kV.

r-θ plane) is given by $\varepsilon = 4r \tan\theta$. The beam brightness is defined as

$$B = \frac{I}{\varepsilon_{\text{norm}}{}^2}, \tag{2}$$

where I is the beam flux. Here, we simulate the brightness assuming the following realistic conditions: (i) the source activity is 3.7 GBq (100 mCi); (ii) the moderator efficiency is 10^{-4}; (iii) $r=2$ mm; (iv) $\Phi_m = 3$ V; and (v) the maximum angular deviation of emitted positrons from the normal direction to the moderator surface is $\sim$100 mrad because of thermal fluctuation. After the beam acceleration up to 10 keV, we get $\varepsilon \sim 14$ mrad mm from Eq. (1). For RHEPD experiments, we may require $\theta = 1$ mrad and $r = 0.5$ mm and hence $\varepsilon = 2$ mrad mm and $\varepsilon_{\text{norm}} = 200$ mrad mm $\text{V}^{1/2}$. Since the total beam efficiency is estimated to be $10^{-4} \times 2/14 \times 1/2 \sim 7 \times 10^{-6}$, the beam flux should be $\sim 2 \times 10^4$ e^+/s. Subsequently, we get $B \sim 5 \times 10^7$ $\text{e}^+/\text{s}/\text{cm}^2/\text{rad}^2/\text{V}$, which is comparable to that of low-energy positrons, using the brightness enhancement technique.[11] It is observed that the beam acceleration makes no essential contribution to obtaining such brightness, since the brightness defined above is normalized to the beam energy.

Considering the above prospect, we designed the beam apparatus as shown in Fig. 1. Radiations from the positron source are shielded with Pb brocks. The positron beam is transported from the gun to the sample chamber through five coaxial magnetic lenses and a 90°-bending magnet. Steering coils are also placed before and after the magnet. A positron source with a nominal activity of 3.7 GBq, which was purchased from the iThemba LABS of South Africa, is installed. Positrons are emitted through a Ti window with a thickness of 5 μm and a radius of 2 mm. A W(100) single crystal with a thickness of 500 nm, obtained from the Arhus University, Denmark, is used as a moderator. An *in situ* annealing of the moderator can be carried out by the direct current flow. Two aperture electrodes with a diameter of 5.8 mm are placed after the moderator. Subsequently, a cylinder electrode with the same aperture diameter is placed. The gap between these electrodes is 2 mm. Finally, an aperture electrode is placed 11 mm from the end of the cylinder electrode. These electrodes are termed as extractor, Wehnelt, Soa, and anode as an analogy to the modified Soa gun. The electrostatic potentials applied to the moderator and electrodes can be varied from 0 V to 20 kV. Only the anode electrode is grounded. To effectively extract slow positrons, taper structures are formed around the peripheries of the moderator and the aperture of extraction electrode.

Figure 2 shows an example of the distribution of electrostatic potential and the beam trajectory simulated using the SIMION program.[12] In this case, the potential of the moderator is 10 kV relative to ground. It is confirmed that the beam is effectively extracted from the moderator and focused once, after the extraction electrode. At the Wehnelt electrode, the electrostatic potential has a saddle point. The beam is well focused by the lens field between the Soa and the anode electrodes. The beam diameter after the anode electrode is reduced to approximately one-third of that of the slow positron generation part.

To avoid beam divergence during transportation, we fabricated conventional magnetic lenses that are covered with yokes. The ampere turn of the coil is 300. The gap length is 15 mm. The magnetic field at the center of the lens is 20 mT when the current is 0.3 A. The focal length in this condition is approximately 150 mm.

Monochromatic positrons are discriminated at the 90°-bending magnet. This bending magnet is also covered with a yoke. The curvature radius is 75 mm. The magnetic field required for the acceleration voltage of 10 kV should be 45 mT. A homogeneous magnetic field (i.e., B_z=constant) focuses the beam in the lateral plane including the central axis. It is necessary to focus the beam in the vertical direction as well. This can be done to form the magnetic field varying in the radial direction, i.e., $B_z/r^{1/2}$. The beam shape is then maintained as axially symmetric, even after passing the bending magnet. To form such a magnetic field, the gap between the two yokes is varied as $22.48 - 0.073r$. Based on the acceptance of the beam port, the energy resolution of the bending magnet is estimated to be ±1 keV.

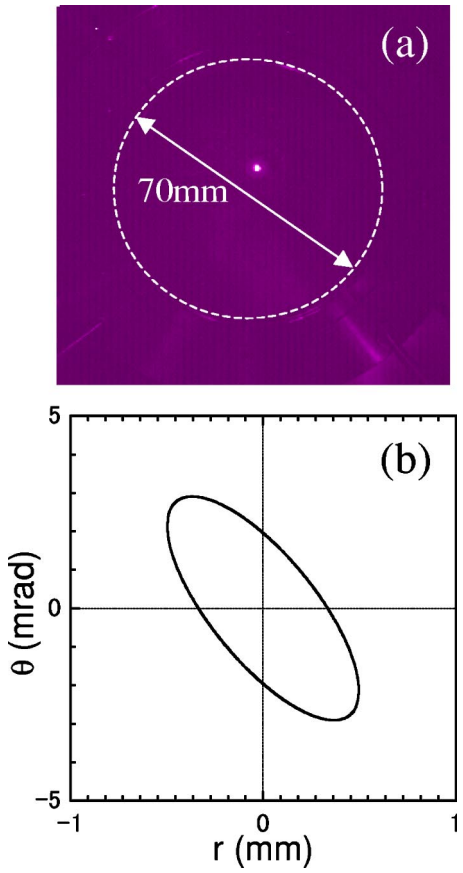

FIG. 3. (Color online) (a) Beam image observed at the sample chamber using a microchannel plate. (b) Phase diagram of the beam obtained by varying the strength of the final magnetic lens when focusing the beam to a 1 mm diameter.

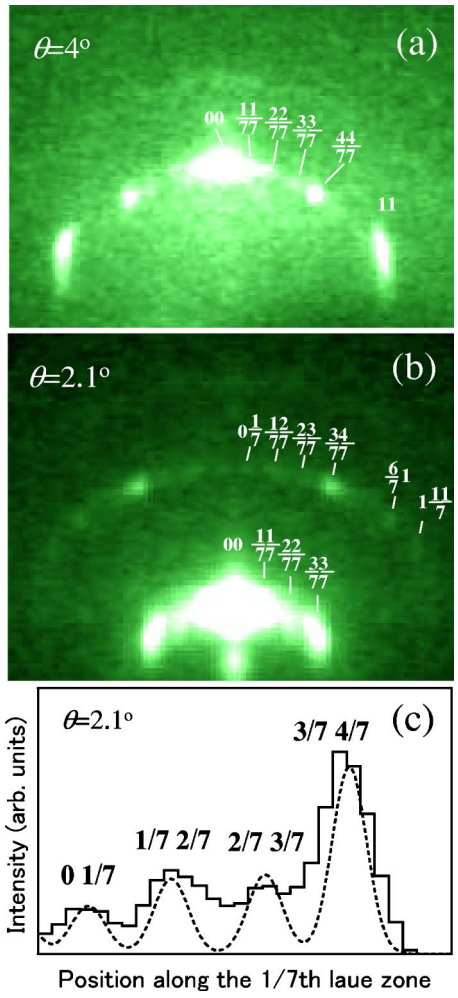

FIG. 4. (Color online) Digitally accumulated RHEPD patterns at the glancing angles of (a) 4.0° and (b) 2.1°. The exposure time is 3 h. Intensity profile along the 1/7-th Laue zone at the glancing angle of 2.1° is shown in (c). A solid line shows the experimental intensity and the broken line shows the theoretical intensity calculated on the basis of the dynamical diffraction theory.

III. BEAM PERFORMANCE AND RHEPD OBSERVATION

Figure 3(a) shows a typical beam image in the target chamber. The beam can be focused below a diameter of 1 mm and it is not observed when the retarding voltage is greater than 10.01 kV. Thus, the energy spread (ΔE) is less than 20 eV (i.e., the energy resolution is 0.2%). The beam flux is determined to be approximately 10^4 e^+/s by measuring the gamma rays with a NaI detector. Assuming the moderator efficiency to be 10^{-4}, the beam transmission efficiency from the moderator to the target stage is estimated to be less than 10%. This agrees well with that estimated in the preceding section based on Liouville's theorem.

We then estimated the emittance and brightness of the beam. Emittance can be determined by measuring the beam size (πr^2) at various focal lengths (f) at the final lens. That is, the beam size is given by

$$\pi r^2 = b\varepsilon L^2[1/f - (1/L - a/b)] + \varepsilon L^2/b^2, \tag{3}$$

where a and b are the Twiss parameters,[13] and L is the distance from the final magnetic lens and the detector. In the so-called "thin-lens approximation," f is given by

$$1/f = 2K^2 d. \tag{4}$$

Here, d is the gap length of the magnetic lens (=15 mm) and K is given by

$$K = \sqrt{\frac{eB^2}{8m\Phi}}, \tag{5}$$

where e is the elemental charge and m is the electron rest mass. Thus, we can determine the Twiss parameters and emittance from πr^2 versus $1/f$ plot. The phase diagram (θ-r space) is given by

$$\theta^2 + \frac{2ar}{b}\theta + \frac{cr^2 - \varepsilon}{b} = 0, \tag{6}$$

where $c=(1+a^2)/b$. Figure 3(b) shows the phase diagram obtained from the above consideration when the beam is focused to 1 mm diameter. The emittance is estimated to be 0.98 π mm mrad. The maximum angular spread is 2.9 mrad. The brightness is obtained as $\sim 10^7$ $e^+/s/cm^2/rad^2/V$. This value is in good agreement with the rough estimation based on the Liouville's theorem in the preceding section. The beam brightness is adequately enhanced without brightness enhancement because of the easy reduction of the beam emittance.

To observe the diffraction pattern, it is important to enhance the coherence length of the positron beam, since it dominates the resolving power. Actually, the coherence length is a more direct measure than brightness and emittance to assure the beam performance in the diffraction experiments. The beam parallel and normal coherence lengths are given by

$$l_p = 1 \Bigg/ \sqrt{\left(\frac{\Delta E}{24.5\sqrt{E}}\right)^2 + \left(\frac{\Delta\theta \sin\theta_g}{\lambda}\right)^2} \tag{7}$$

and

$$l_n = \lambda/\Delta\theta, \tag{8}$$

respectively.[14] Here, $\Delta\theta$ and λ are the angular spread and wavelength of the beam, respectively, θ_g is the glancing angle of positron beam to the surface. For the present beam, we get $l_p \sim 120$ Å at and $l_n \sim 40$ Å. These are long enough to observe the reconstructed surface with a large unit cell.

We performed the RHEPD experiments using a Si(111)-7×7 reconstructed surface. Figure 4 shows the RHEPD patterns from a Si(111)-7×7 surface at the glancing angles of 2.1° and 4° which satisfy the primary and fourth Bragg conditions, respectively. It is found that the fractional-order diffraction spots are clearly seen as indicated. The pattern quality had fairly improved from the previously obtained one using the electrostatic beam system.[15] In Fig. 4(c), it is confirmed that the observed intensity profile along the 1/7-th Laue zone agrees well with that calculated by the dynamical diffraction theory.

Thus, the present beam using electromagnetic lenses is very suitable to RHEPD experiments. A quantitative analysis of RHEPD patterns is also possible.

ACKNOWLEDGMENT

This work was partly promoted by the Nuclear Energy Fundamentals Crossover Research in the Ministry of Education, Culture, Sports, Science and Technology, of Japan.

[1] A. Kawasuso and S. Okada, Phys. Rev. Lett. **81**, 2695 (1998).
[2] A. Kawasuso, T. Ishimoto, Y. Fukaya, K. Hayashi, and A. Ichimiya, J. Surf. Sci. Nanotechnol. **1**, 152 (2003).
[3] A. Ichimiya, Solid State Commun. **28–29**, 143 (1992).
[4] A. Kawasuso, S. Okada, and A. Ichimiya, Nucl. Instrum. Methods Phys. Res. B **171**, 219 (2000).
[5] T. Ishimoto, A. Kawasuso, and H. Itoh, Appl. Surf. Sci. **194**, 43 (2002).
[6] A. Kawasuso, T. Ishimoto, S. Okada, H. Itoh, and A. Ichimiya, Appl. Surf. Sci. **194**, 287 (2002).
[7] K. F. Canter, P. H. Lippel, W. S. Crane and, A. P. Mills, Jr., in *Positron Studies of Solids, Surfaces, and Atoms*, edited by A. P. Mills, Jr., W. S. Crane, and K. F. Canter (World Scientific, Singapore, 1986), p. 199.
[8] F. A. Selim, A. W. Hunt, J. A. Golovchenko, R. H. Howell, R. Haakeenaasen, and K. G. Lynn, Nucl. Instrum. Methods Phys. Res. B **171**, 182 (2000).
[9] A. P. Mills, Jr., Appl. Phys. **23**, 189 (1980).
[10] K. Canter, Can. J. Phys. **60**, 551 (1982).
[11] G. R. Brandes, K. F. Canter, T. N. Horsky, P. H. Lippel, and A. P. Mills, J. Phys.: Condens. Matter **1**, SA135 (1989).
[12] D. A. David, EG&G Idaho National Engineering Laboratory.
[13] H. Wollnik, *Optics of Charged Particle* (Academic, New York, 1987), Chap. 5, pp. 151–156.
[14] G. Comsa, Surf. Sci. **81**, 57 (1979).
[15] A. Kawasuso, Y. Fukaya, K. Hayashi, M. Maekawa, S. Okada, and A. Ichimiya, Phys. Rev. B **68**, 241313 (2003).